

Figure S1. Selectivity of the C-LTMRs deletion in the DRG and the DHSC

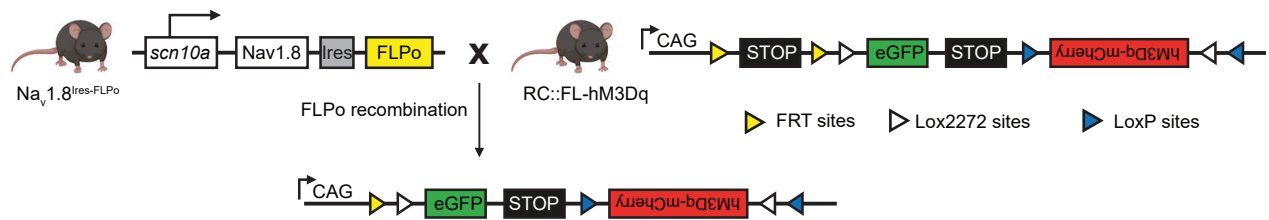
(A) Representative images of lumbar (L3) DRG sections stained with cell type markers in control and *C-LTMRs-DTR* mice. Scale bar: 100 μ m.

(B) Quantification of the total number of lumbar (L3) CGRP⁺ DRG neurons (t-test) and P2X3⁺ DRG neurons (Mann Witney test) in control (n=5) and *C-LTMRs-DTR* mice (n=6). Data are presented as mean \pm SEM. Dots represent individual animals.

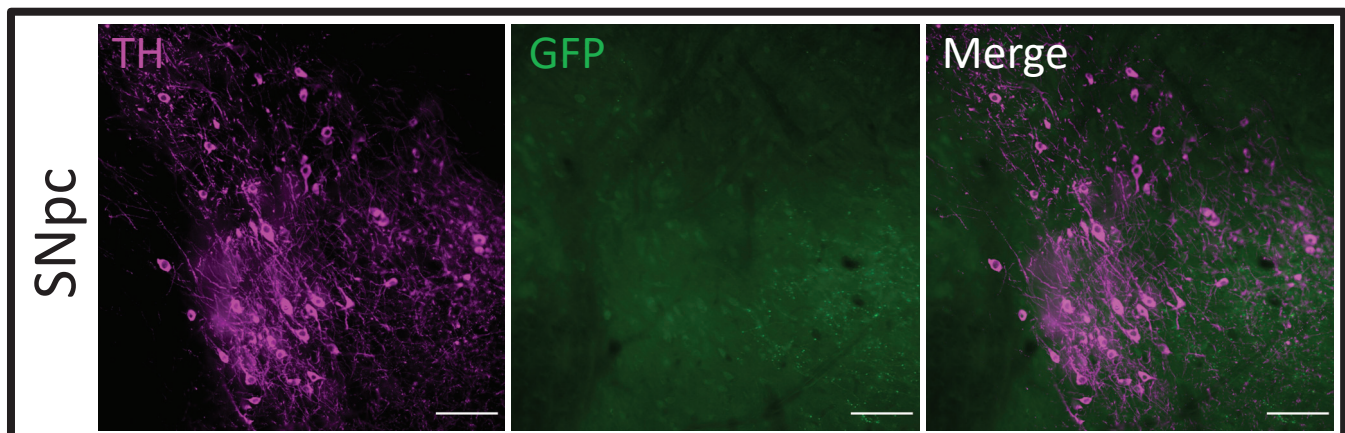
(C) Top: Lumbar segments of the dorsal horn of the spinal cord from control and *C-LTMRs-DTR* mice immunolabeled for CGRP (red), IB4 (blue) and VGLUT3 (green). Bottom: Zoom-in view of the selected areas in top. Scale bar: 100 μ m.

(D-E) Quantification of (D) non-labelled GIa glomeruli and (E) IB4⁺ glomeruli in the DHSC, in control (n=5) and *C-LTMRs-DTR* mice (n=6). Data are presented as mean \pm SEM. Dots represent individual animals. Statistical comparisons were performed using t-test, *P < 0.05 et ***P < 0.0001.

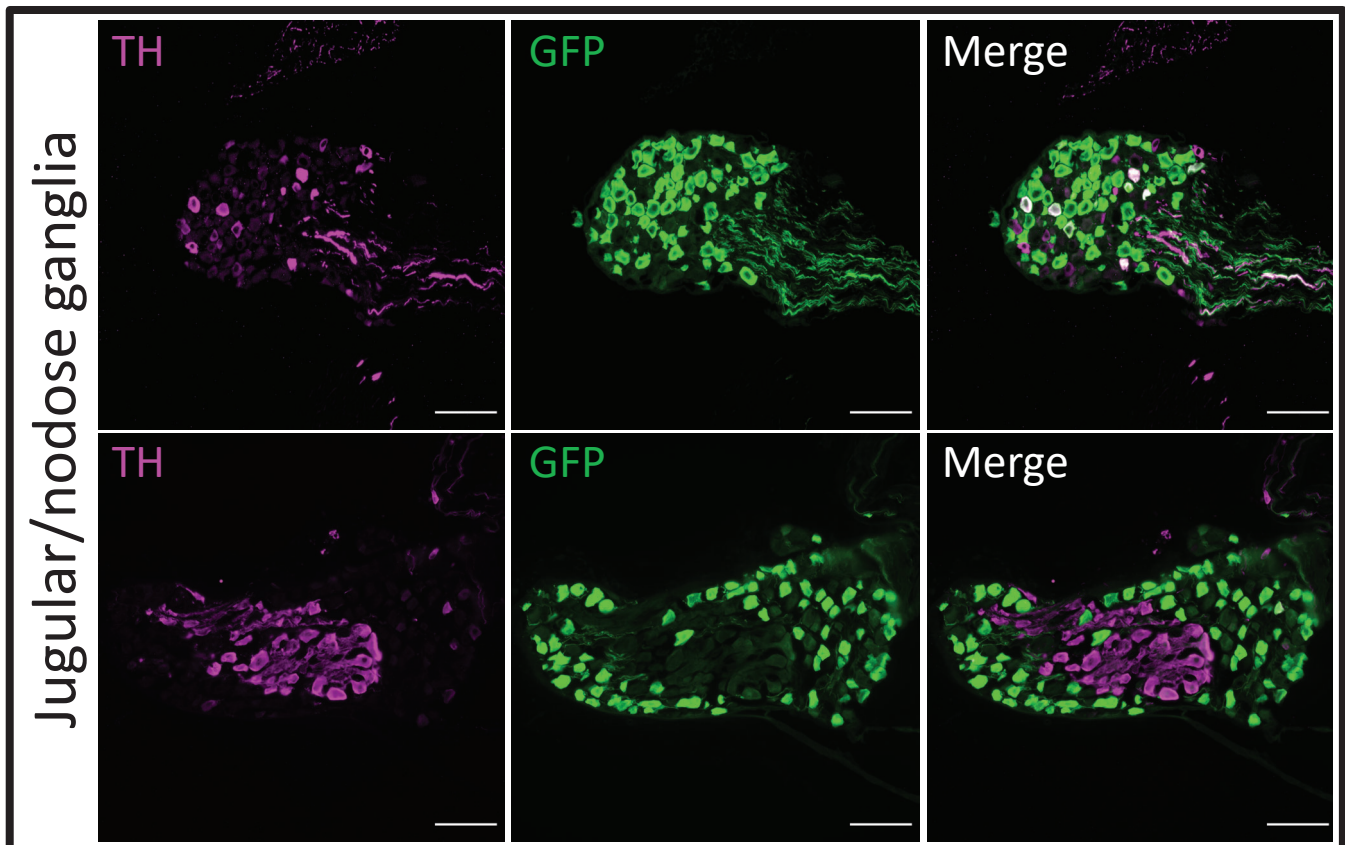
A



B



C



D

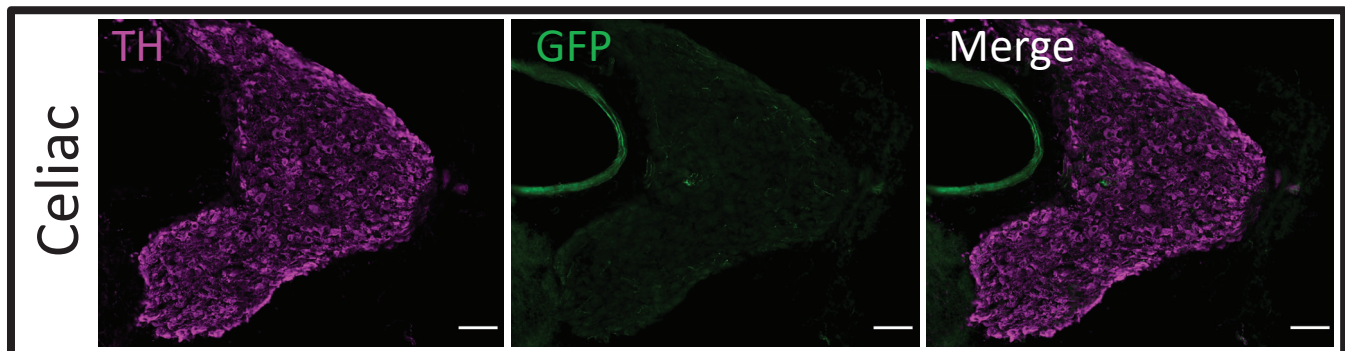
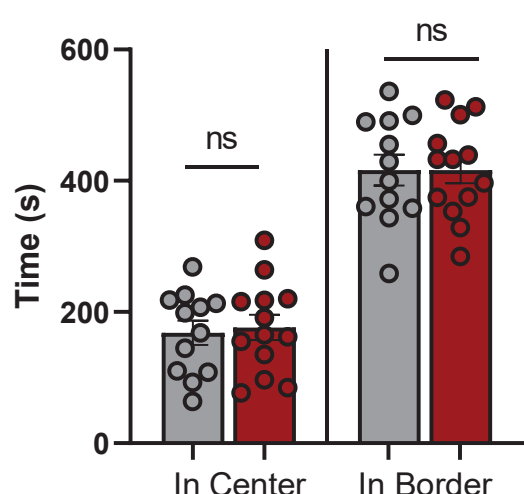


Figure S2. Selectivity of the Nav1.8-TH signature to C-LTMRs

(A) Schematic representation of the strategy for mating between a $\text{Nav1.8}^{\text{Ires-FLP}^0}$ mouse and a reporter RC::FL-hM3Dq mouse. In the progeny of this cross, the FLP⁰ excises the FRT-flanked transcription STOP cassette, allowing the expression of EGFP in the Nav1.8 lineage cells.

(B–D) TH (magenta) and GFP (green) immunostaining on (B) sagittal brain section at the level of the Substantia Nigra pars compacta (SNpc), (C) jugular-nodose-ganglia (JNG) section and (D) Celiac ganglion section from a $\text{Na}_v1.8^{\text{Ires-FLP}^0} :: \text{RC-FL-hM3Dq}$ mouse. Scale bar: 100 μm .

A

Open field

B

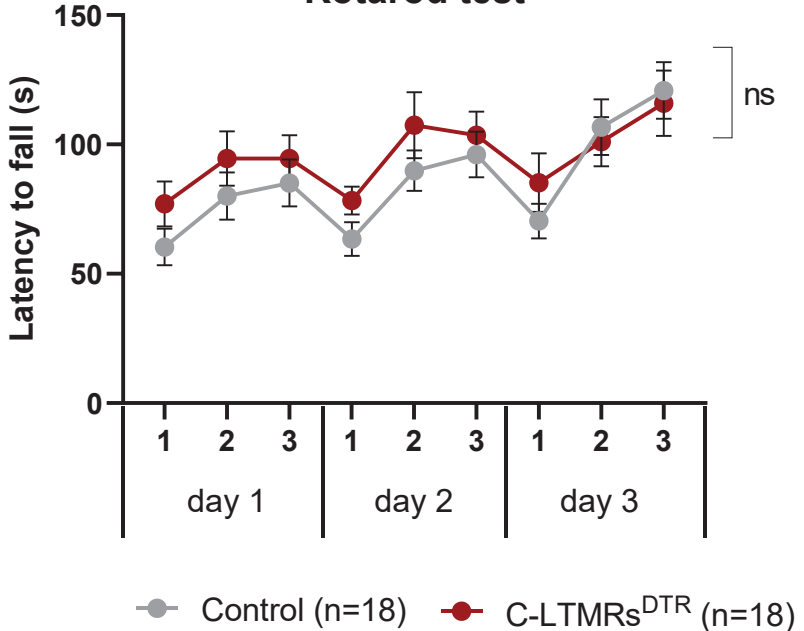
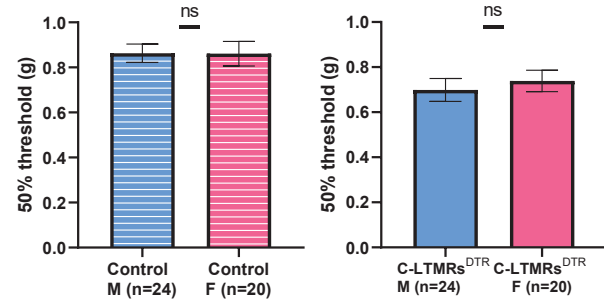
Rotarod test

Figure S3. Partial C-LTMRs ablation does not induce anxiety behavior or disturbances in sensorimotor coordination

(A-B) *C-LTMRs-DTR* mice display unaltered phenotype compared to control mice in (A) anxiety with openfield test (n=12 control, n=13 *C-LTMRs-DTR*) and (B) in motor coordination with rotaroad test (n=18 in each group)

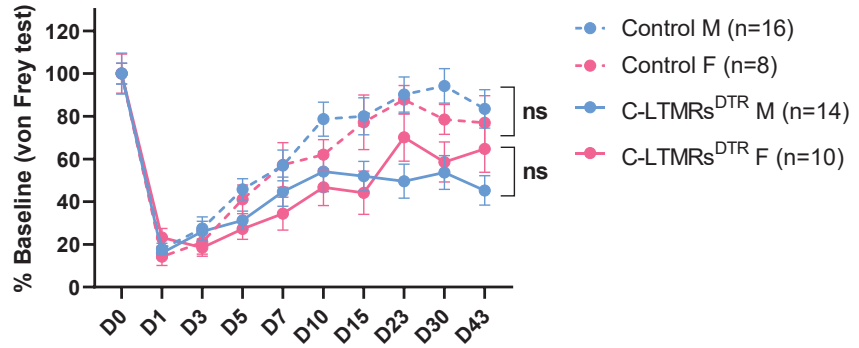
A

Von Frey_Baseline



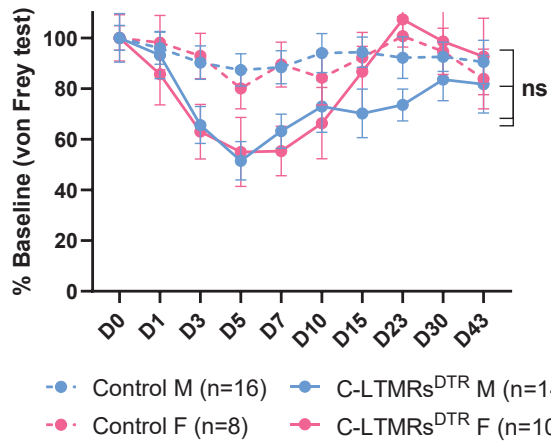
B

Paw incision_ipsi



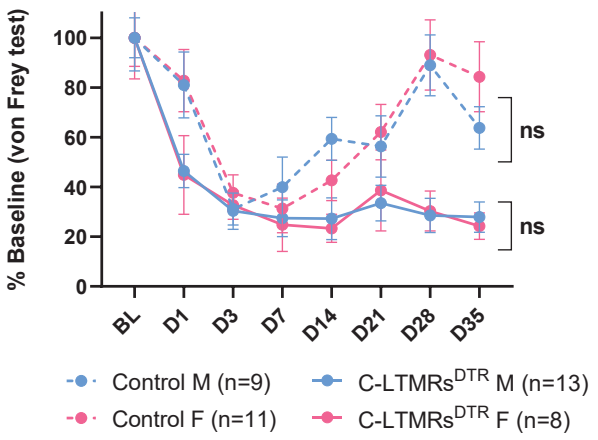
C

Paw incision_contra



D

Paclitaxel



E

Dry Ice Test_Baseline

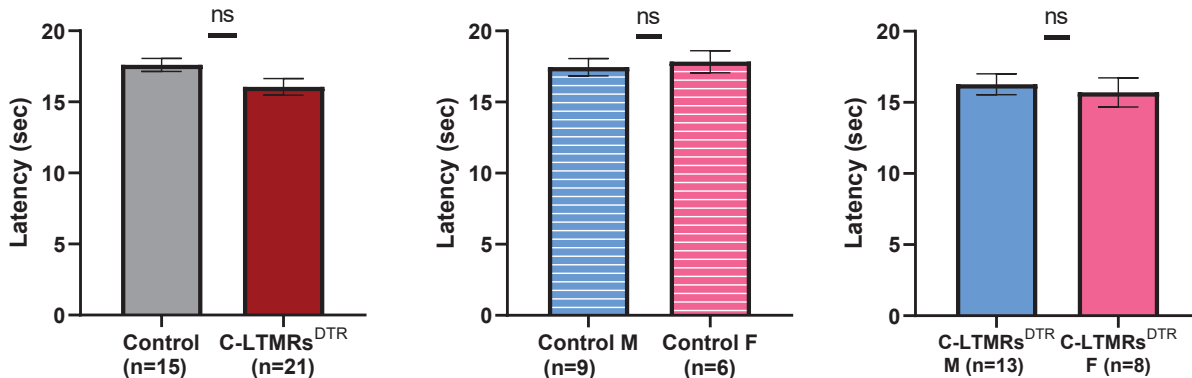


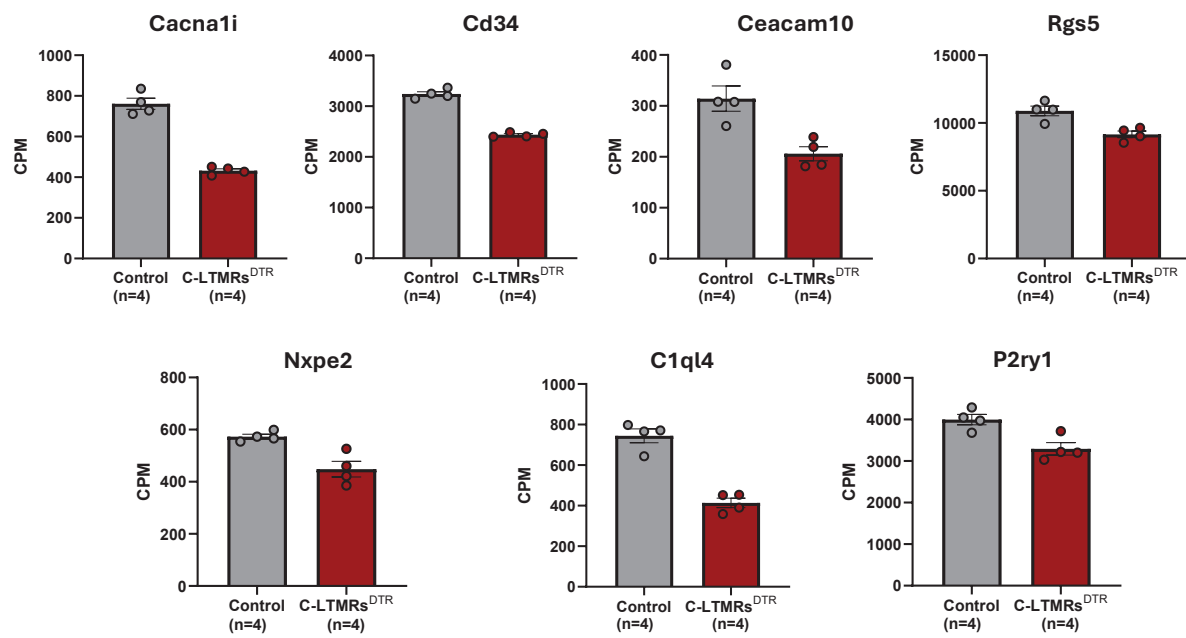
Figure S4. Males and Females of both genotypes display no differences for mechanical and cold plantar sensitivity in naive conditions and following injury

(A) Baseline mechanical thresholds measured by Von Frey testing show no differences between males (n=24) and females (n=20) of both genotypes (unpaired t-test).

(B-D) Males and females of both genotypes behave in a similar manner across all time point in terms of mechanical sensitivity of (B) the ipsi or (C) the contralateral side before and following paw incision and (D) before and following paclitaxel. Results are expressed as mean \pm SEM for indicated mice number (two-way repeated measures ANOVA).

(E) No differences are observed between control (n=15) and *C-LTMRs-DTR* mice (n=21) in terms of cold sensitivity, at the baseline level. Males and females of both genotypes behave in a similar manner. Results are expressed as mean \pm SEM for indicated mice number (unpaired t-test).

A



B

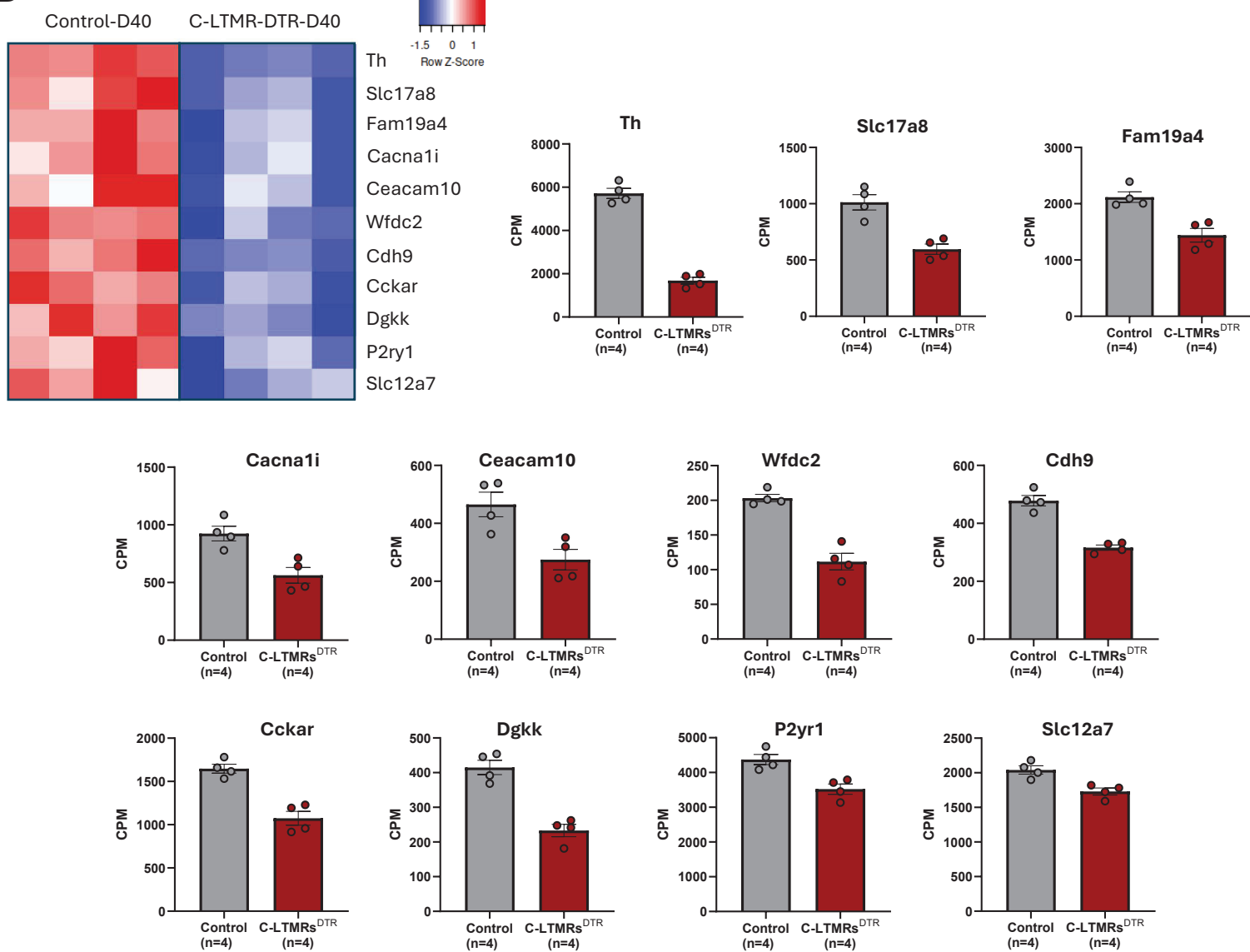


Figure S5. *C-LTMRs-DTR* mice exhibit a drastic decrease in the expression of many C-LTMRs-specific and enriched genes

(A) Counts Per Million (CPM) obtained after RNA-Seq for the C-LTMR-specific and enriched genes presented in Fig.4A, in control (gray) and *C-LTMRs-DTR* (red) mice. Results are expressed as mean \pm SEM for indicated mice number. Dots represent individual animals.

(B) Heatmap representing the expression of indicated C-LTMRs-specific and enriched genes in control and *C-LTMRs-DTR* mice, 40 days following paw incision; and graphical representations of the level of expression (CPM) of these genes. Results are expressed as mean \pm SEM for indicated mice number. Dots represent individual animals.

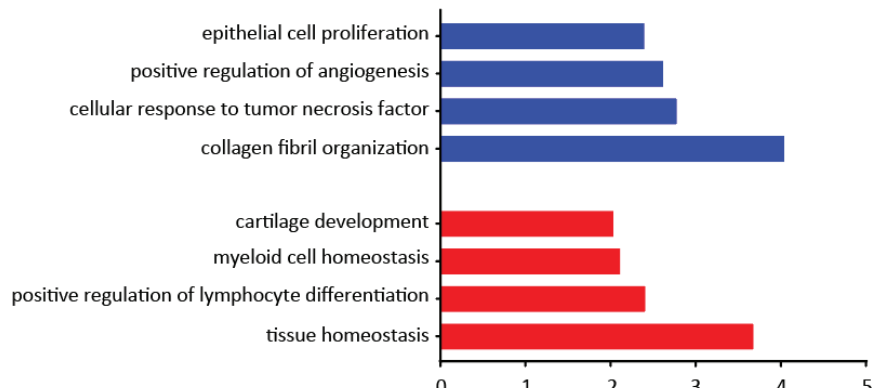
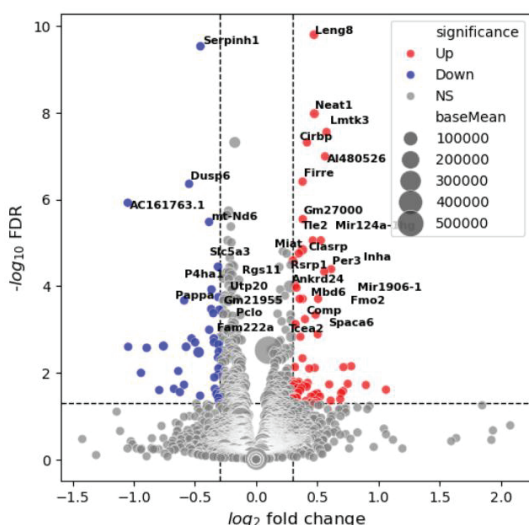
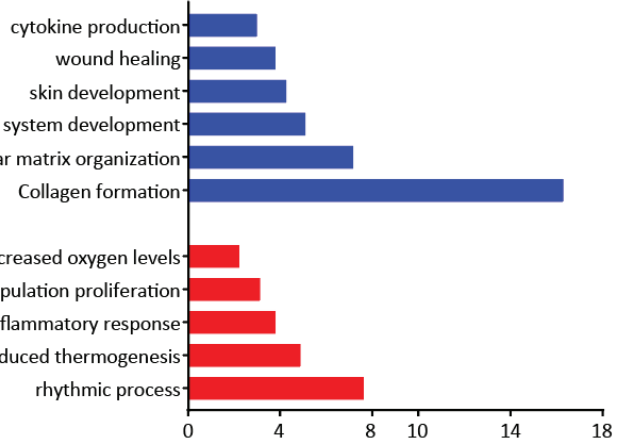
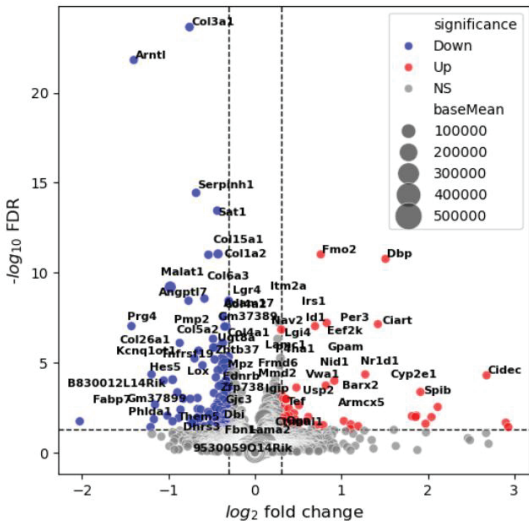


Figure S6. Partial depletion of C-LTMRs modifies DRG response to paclitaxel

(A) Volcano plot representing up- and down-regulated DEG in the L3-L5 DRGs at day 40 (D40) after paclitaxel administration as compared to untreated (D0) control mice (FDR5, Log2FoldChange > 0.3, n=4 samples per genotype).

(B) Up (red) and down (blue)-regulated biological processes and pathways in control lumbar DRGs at D40 after paclitaxel administration, determined with Metascape software.

(C) Volcano plot representing up- and down-regulated DEG in the L3-L5 DRGs at day 40 (D40) after paclitaxel administration as compared to untreated (D0) *C-LTMRs-DTR* mice (FDR5, Log2FoldChange > 0.3, n=4 samples per genotype).

(D) Up (red) and down (blue)-regulated biological processes and pathways in *C-LTMRs-DTR* lumbar DRGs at D40 after paclitaxel administration, determined with Metascape software.

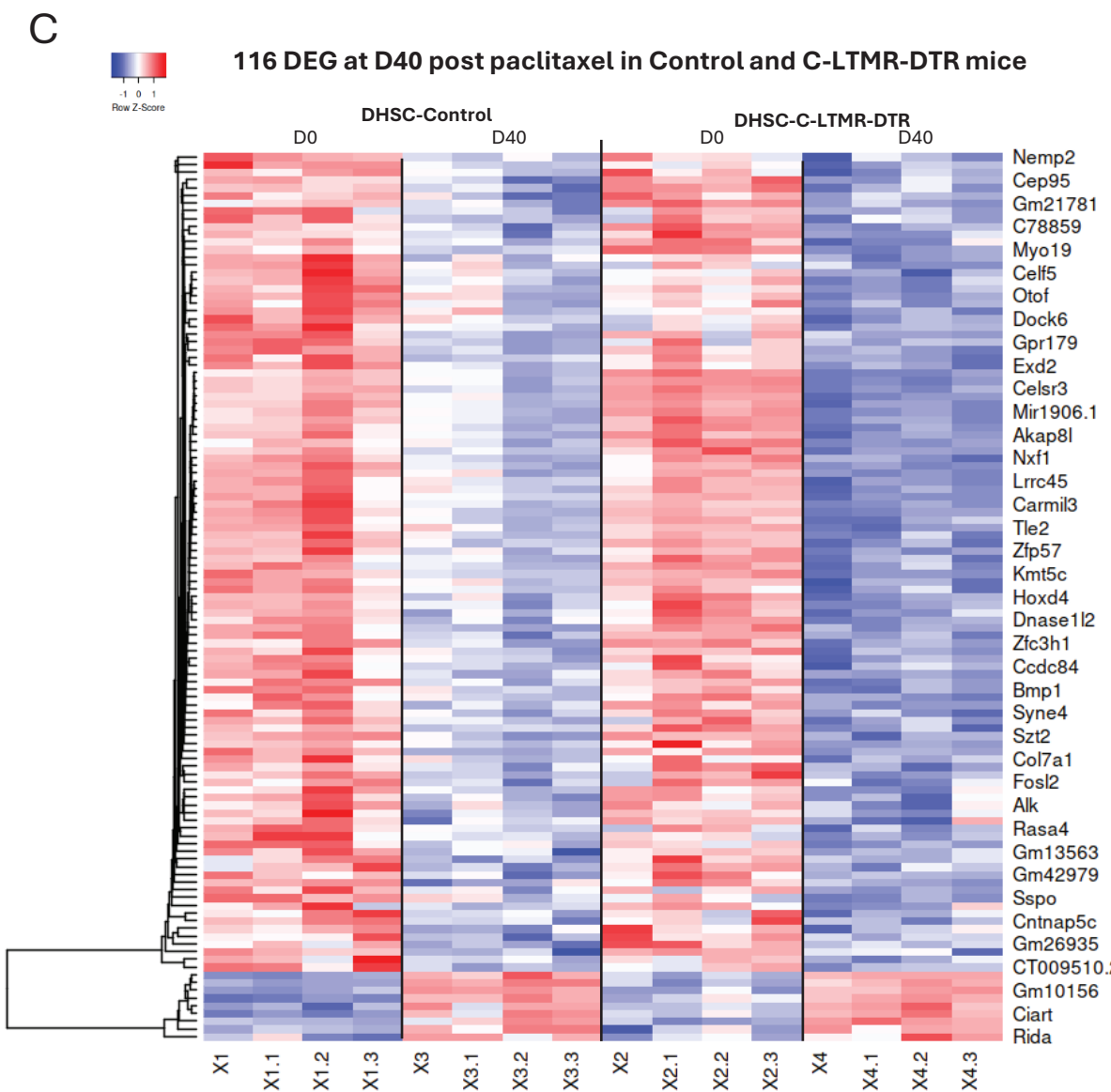
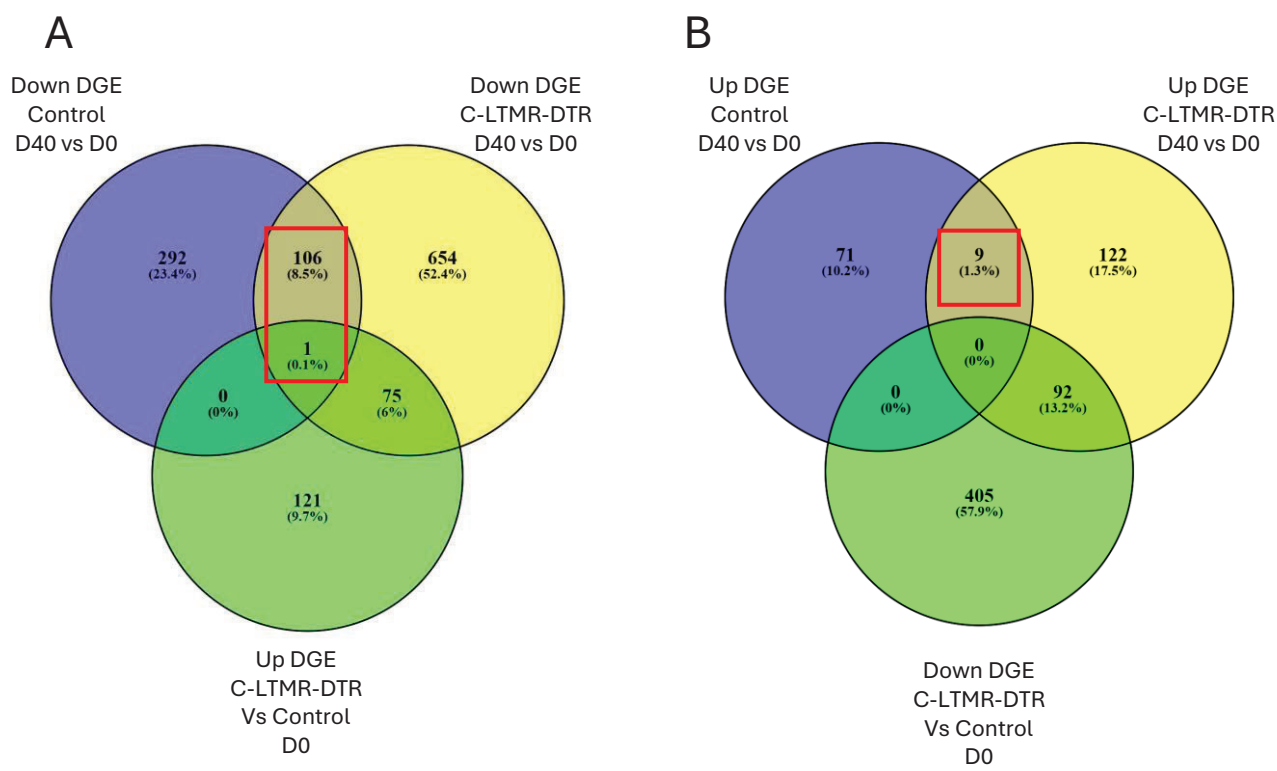


Figure S7. Analysis of RNA-Seq data from DHSC to identify the sets of genes similarly affected by paclitaxel in controls and *C-LTMRs-DTR* mice

(A-B) Venn diagrams were used to compare the sets of down and up DEG identified in the D40 vs D0 comparison in control and *C-LTMRs-DTR* DHSC (FDR5, Lod2FoldChange >0.3, n=4 samples per experimental group). To identify the genes whose de-regulation was due to paclitaxel but not to the differences observed in naïve condition between *C-LTMRs-DTR* and control DHSC, the indicated sets of DEG at day 0 were included in the Venn diagram. Red rectangle shows the sets of genes (107) down and up (9)-regulated in both control and *C-LTMRs-DTR* at day 40 after paclitaxel.

(C) Heatmap representing the expression levels of these 116 DEG which are common to both control and *C-LTMRs-DTR* DHSC in each indicated experimental group.

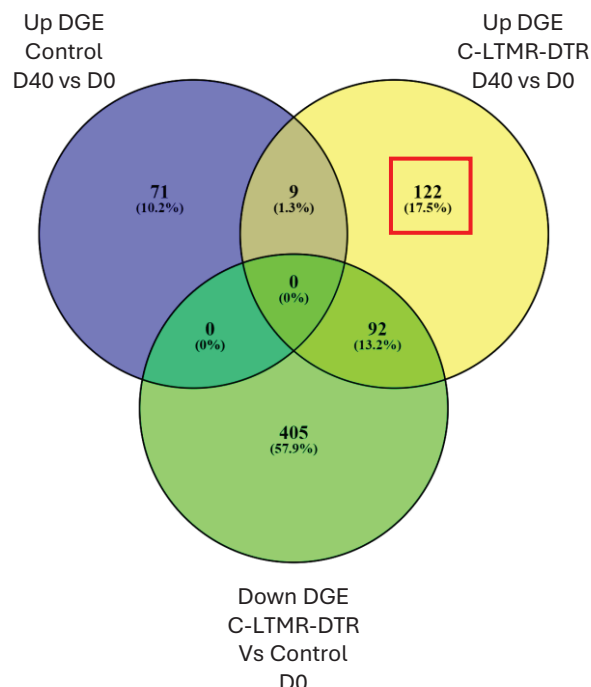
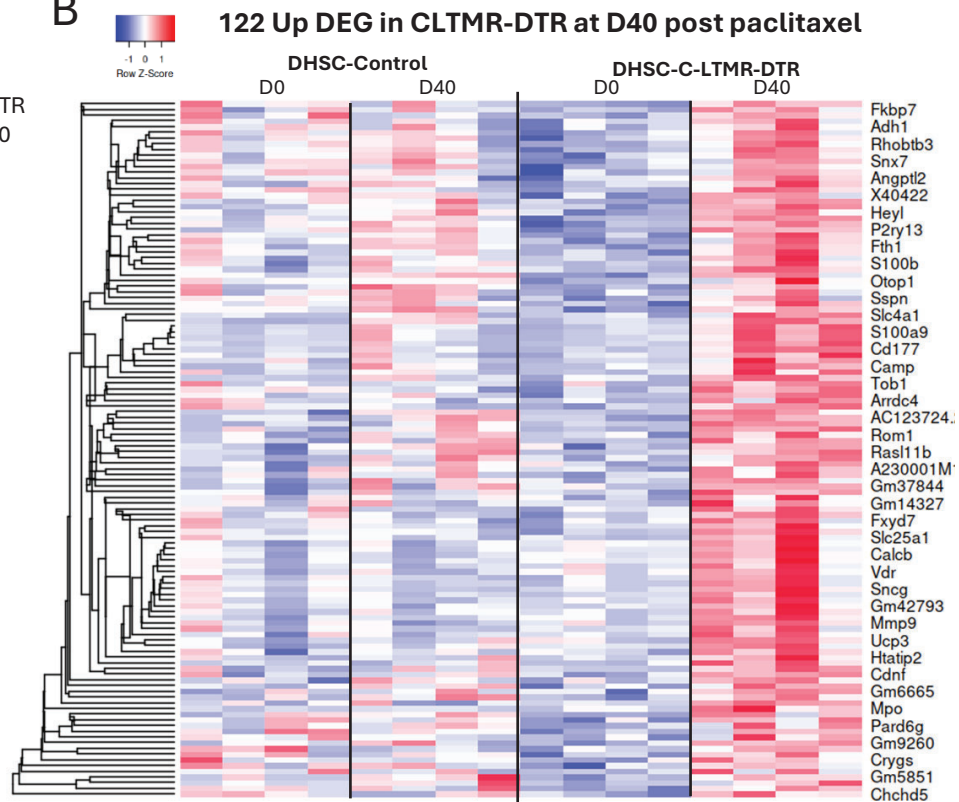
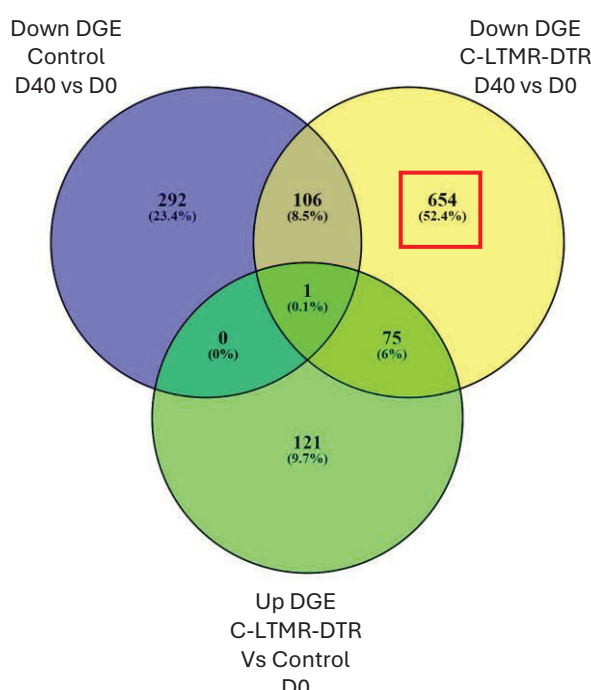
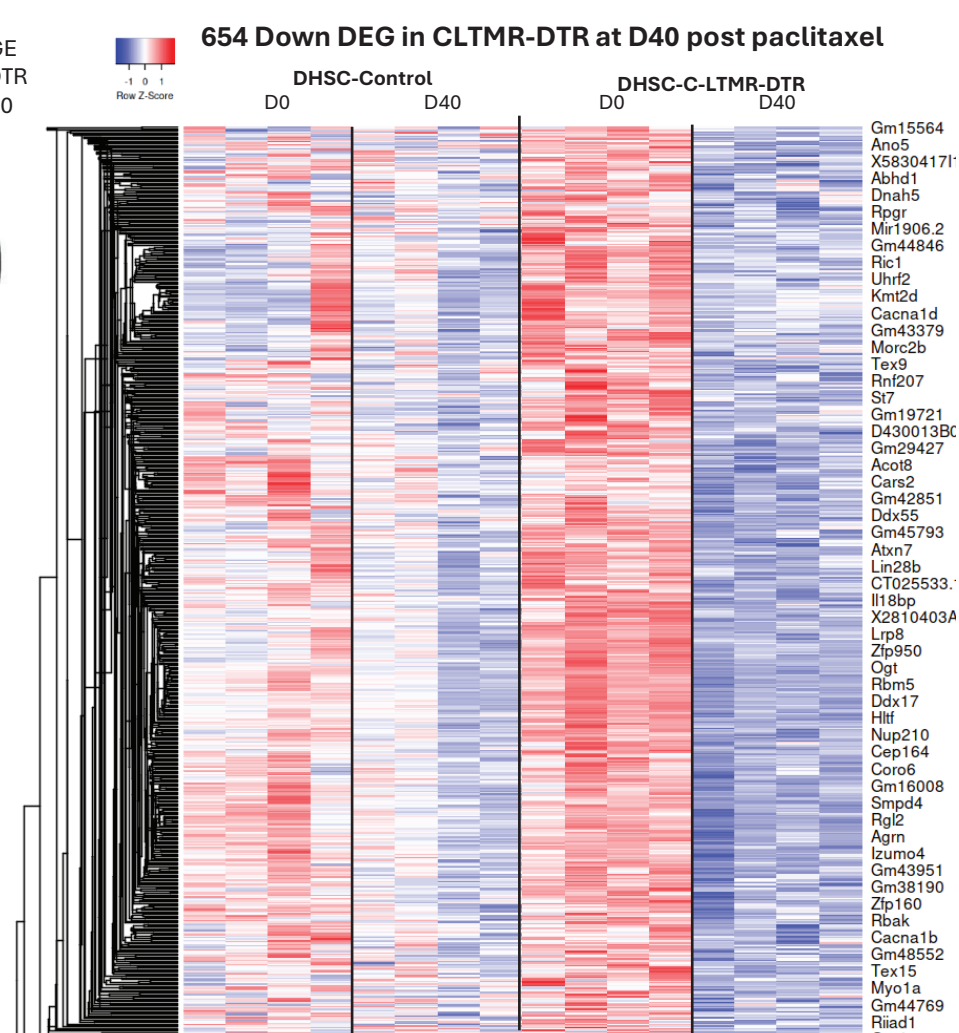
A**B****C****D**

Figure S8. Analysis of RNA-Seq data from DHSC to identify the sets of genes uniquely disrupted in *C-LTMRs-DTR* mice

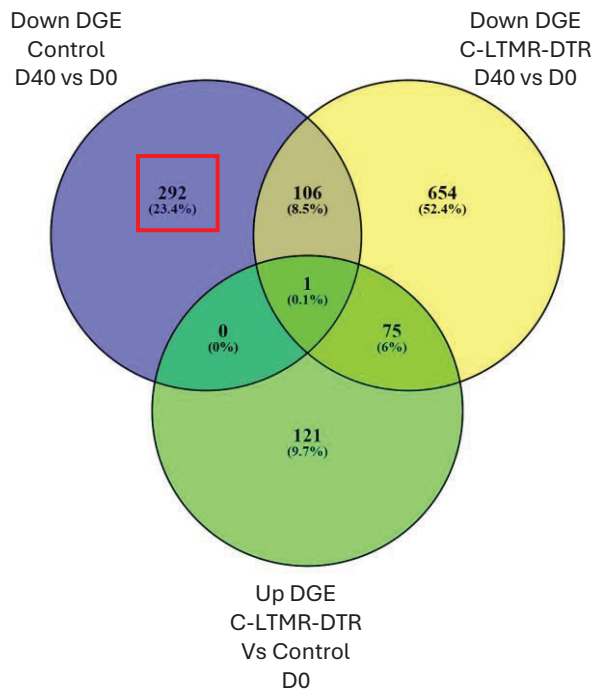
(A) Venn diagrams were used to compare the sets of down and up DEG identified in the D40 vs D0 comparison in control and *C-LTMRs-DTR* DHSC (FDR5, Lod2FoldChange >0.3, n=4 samples per experimental group). 122 up-regulated genes in *C-LTMRs-DTR* DHSC at D40 after paclitaxel (D40 vs D0) were identified by excluding those that were common with control up-DEG D40 vs D0 and those that were already down-regulated at day 0 in *C-LTMRs-DTR* as compared to control mice.

(B) Heatmap projection of these 122 genes across experimental groups.

(C) 654 down-regulated genes in *C-LTMRs-DTR* DHSC at D40 after paclitaxel (D40 vs D0) were identified by excluding those that were in common with control down-DEG D40 vs D0 and those that were already up-regulated at day 0 in *C-LTMRs-DTR* as compared to control mice.

(D) Heatmap projection of these 654 genes across experimental groups.

A



B

292 Down DEG in Control at D40 post paclitaxel

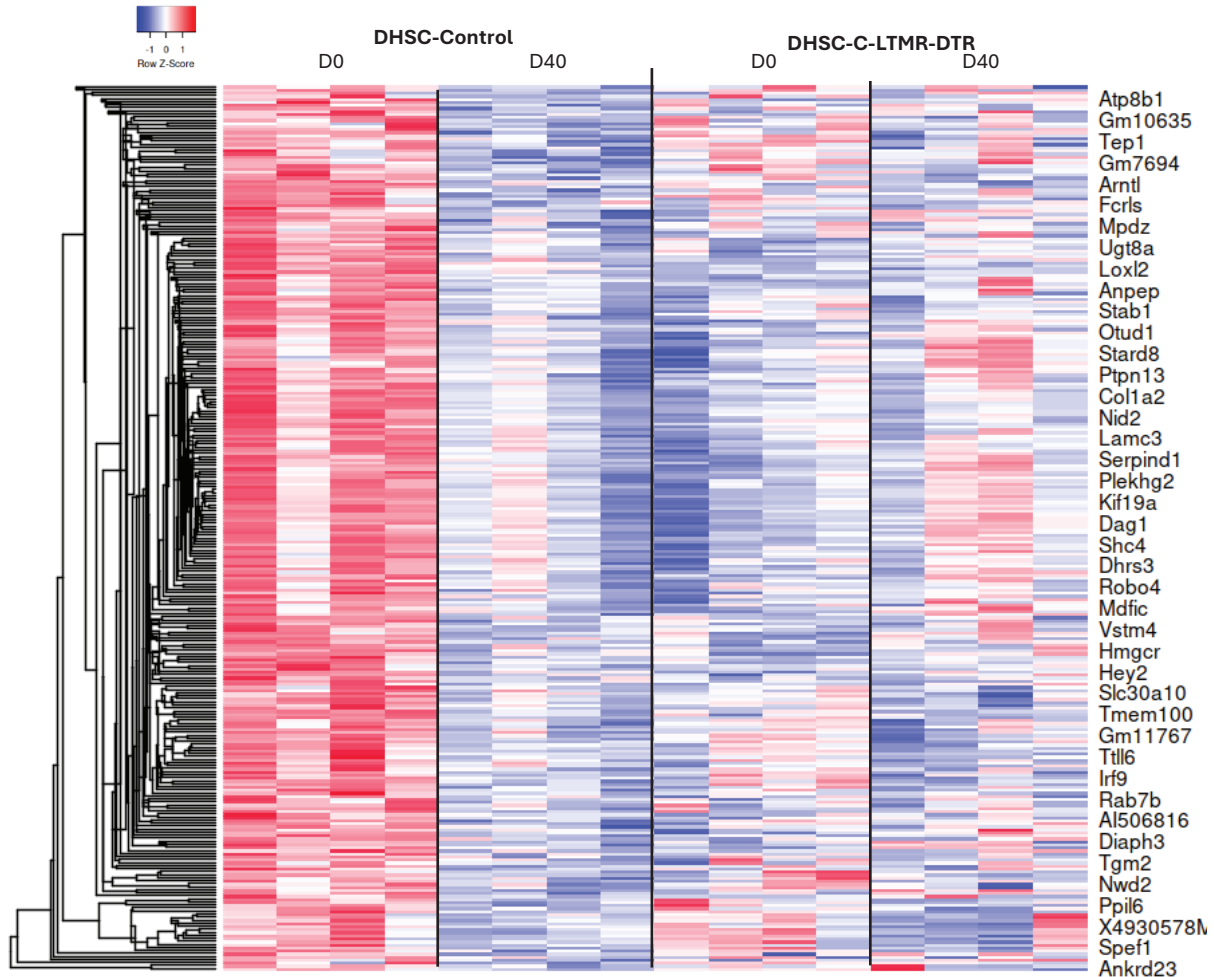


Figure S9. Analysis of RNA-Seq data from DHSC to identify the sets of genes suppressed in control mice in response to paclitaxel administration

(A) Venn diagrams were used to compare the sets of down and up DEG identified in the D40 vs D0 comparison in control and *C-LTMRs-DTR* DHSC (FDR5, Lod2FoldChange >0.3, n=4 samples per experimental group). 292 genes were identified as being selective to the control D40 vs D0 condition.

(B) Heatmap projection of these 292 genes across experimental groups.